

**PETROGRAPHY AND MINERAL CHEMISTRY OF TOURMALINE IN MOLLA TALEB GRANITOID, NORTHEAST OF ALIGUDARZ (LORESTAN PROVINCE)****PETROGRAFIA E QUÍMICA MINERAL DE TURMALINA NO GRANITOIDE MOLLA TALEB, NO NORESTE DE ALIGUDARZ (PROVINCIA DE LORESTAN)**Davoud Pirdadeh Beyranvand<sup>1</sup>Afshin Ashja Ardalan\*<sup>2</sup>Taher Farhadinejad<sup>3</sup>Mohammad Ali Arian<sup>4</sup>**ABSTRACT**

Molla Taleb pegmatites (northeast of Aligudarz) are located in the western part of the metamorphic-igneous Sanandaj-Sirjan Zone (SSZ). Slates and schists along with siliceous veins and veinlet and black Hornfels, as well as metamorphic sandstones are among the oldest deposits of this area. The most important geological event in this area is the development and intrusion of granitoid masses into schists of the Molla Taleb area during the Middle Jurassic. The rocks of the study area are in the range of gabbro, diorite, granodiorite, and granite. Granites are in the range of type-I granites. Most specimens are calc-alkaline and mainly contain peraluminous. Microprobe electron analysis of tourmalines present in pegmatites, tourmaline- aplite-pegmatite veins, nodular tourmalines, and quartz-tourmaline veins shows that all tourmalines are in the Schorl region and the range of alkaline tourmalines. These tourmalines with FeO / FeO + MgO ratios between 0.6 and 0.8 are in the range of magmatic-hydrothermal tourmalines and more than 0.8 in the magmatic range. Therefore, the studied tourmalines are dependent on granite environments and are formed by a hydrothermal fluid of magmatic origin.

**KEYWORDS:** TOURMALINE; CALC-ALKALINE; GRANITE; MICROPROBE ANALYSIS; MOLLA TALEB; ALIGUDARZ; SANANDAJ-SIRJAN ZONE.

As pergamitas de Molla Taleb (noroeste de Aligudarz) estão localizadas na parte ocidental da Zona Sanandaj-Sirjan área metamórfica-ígnea (SSZ). Os xistos compostos de veios siliciosos e veios pretos e Hornfels, bem como arenitos metamórficos estão entre os depósitos mais antigos desta área. O evento geológico mais importante nesta área foi o desenvolvimento e intrusão de massas granitóides na área xistosa de Molla Taleb durante o Jurássico Médio. As rochas da área de estudo estão na faixa de gabro, diorito, granodiorito e granito. Os granitos estão na faixa dos granitos do

<sup>1</sup>Department of Geology, Faculty of Science, North Tehran Branch, Islamic Azad University, Tehran, Iran [pbdavoud@gmail.com](mailto:pbdavoud@gmail.com) ORCID: <https://orcid.org/0000-0001-9879-0028>

<sup>2</sup>Assistant Professor, Department of Geology, North Tehran Branch, Islamic Azad University, Tehran, Iran

\*Corresponding autor. [afshinashjaardalan@yahoo.com](mailto:afshinashjaardalan@yahoo.com) ORCID: <https://orcid.org/0000-0002-1800-9594>

<sup>3</sup> Soil Conservation and Watershed Management Research Department, Lorestan Agricultural and Natural Resources Research and Education Center, AREEO, Khoramabad, Iran. [farhadinejad@gmail.com](mailto:farhadinejad@gmail.com) ORCID: <https://orcid.org/0000-0001-9263-1608>

<sup>4</sup>Associate Professor, Department of Geology, North Tehran Branch, Islamic Azad University, Tehran, Iran. [m-arian@iau-tnb.ac.ir](mailto:m-arian@iau-tnb.ac.ir) ORCID: <https://orcid.org/0000-0001-8193-0274>

tipo I. A maioria das amostras são calco-alcalinhas e contêm principalmente peraluminosos. Uma análise dos elétrons com uma microsonda das turmalinas presentes nos pegmatitos, demonstraram os veios turmalina-aplito-pegmatita, a turmalina nodular e os veios quartzo-turmalina mostram que todas as turmalinas se encontram na região de Schorl e não na gama da turmalina alcalina. Estas turmalinas com razões  $\text{FeO} / \text{FeO} + \text{MgO}$  entre 0,6 e 0,8 não estão na faixa das turmalinas magmático-hidrotérmicas e mais de 0,8 na faixa magmática. As turmalinas estudadas dependem de ambientes graníticos e são formadas por um fluido hidrotérmico de origem magmática.

**KEYWORDS:** TURMALINA; CALC-ALCALINO; GRANITO; ANÁLISES COM MICRO SONDAS; MOLLATALEB; ALIGUDARZ; REGIÃO SANANDAJ-SIRJAN.

## INTRODUCTION

Tourmaline is one of the important accessory minerals in pegmatites and aplites. Henry (1999) characterizes the crystalline structure of this aqueous borosilicate mineral as  $\text{XY}_3\text{Z}_6(\text{T}_6\text{O}_{18})(\text{BO}_3)_3$ . In this structure, position X contains Ca, Na, and K and position Y is occupied by various substitutions of the mono- to four valent cations Li, Mg,  $\text{Fe}^{2+}$ ,  $\text{Mn}^{2+}$ , Al,  $\text{Cr}^{3+}$ ,  $\text{V}^{3+}$ ,  $\text{Fe}^{3+}$ , or  $\text{Ti}^{4+}$ . Position Z is filled with Al and sometimes with  $\text{Fe}^{2+}$ ,  $\text{V}^{3+}$ , Cr, Mg, Ti,  $\text{Fe}^{3+}$ . Finally, position T is often filled by Si, Al, and B, position W by O, OH, and position V by OH, O, or F (Foit, Rosenberg, 1977). The complex compounds of tourmaline reflect chemical and physical changes in the environment. The complexity of the chemical composition and the very high ability of tourmaline to replace various elements in its structure have led to an increase in the strength and stability of the tourmaline mineral at variable temperature and pressure. Therefore, this mineral can be important as a petrogenetic identifier in recognizing igneous, sedimentary, and metamorphic rocks (Abu El-Enen, Okruc, 2007). Crystallization of this mineral can occur in the transition conditions from the magmatic delayed sub-solidus stage to the initial sub-solidus (Buriánek, Novák, 2007). Tourmaline is formed in a variety of geological environments and is a common mineral in granitic pegmatites, weak to strong metamorphic rocks, and detrital sedimentary rocks. To study the formation and stability of tourmaline and the general composition of host rock and other associated minerals, the study of various factors such as temperature, pressure, oxygen fugacity, boron content, alkalinity, and activity of elements such as Ti, Mg, Fe, Al, and  $\text{H}_2\text{O}$  is of particular importance (Scaillet *et. al.*, 1995; Wolf, London, 1997, Baratian *et. al.*, 2020). Based on optical properties such as color, multicolor, hardness, and chemical composition, five possible sources of

granitic, pegmatite, pegmatite injected in metamorphic areas, autogenic sedimentary tourmalines, and tourmalines of older areas have been proposed for tourmaline (Krynine, 1946). Systematic changes can also be observed in many rare elements in tourmaline mineral based on the type of host rock (Copjakova *et. al.*, 2013). Tourmaline is the major carrier of boron in crustal rocks (Torres-Ruiz *et. al.*, 2003). The composition of tourmalines indicates the composition of the fluid from which they are crystallized (Slack, Trumbull, 2011). This potential is not well known for rare elements in tourmaline (Van Hinsberg, 2011). The pattern of REEs can indicate the geochemistry setting of and processes affecting fractional crystallization and magma fractionation. This is true also for Tourmalines. In pegmatites, the difference in the behavior of related rare elements is in the way they form and whether they can lead to fractional crystallization or partial melting. Fractional crystallization mobilizes incompatible elements in the melt section and compatible elements in the depleted melt section (Michael *et. al.*, 2013). In the partial melting process, the behavior of rare elements is highly dependent on the lithology and the presence or absence of specific accessory minerals, especially biotite (Bea *et. al.*, 1994). Pegmatites resulting from fractional crystallization have more Rb, Be, Li, and Zn and less V and Sr than pegmatites created from partial melting (Michael, *et. al.* 2013). Tourmalines in granites have higher Th, Ph, REE, Ta, Nb, Li, Zn, and U and lower V, Sr, Co, Sc, and Ni than metavolcanics (Galbraith *et. al.*, 2009). In Iran, tourmaline formation has been reported in granite massifs of different regions, including Mashhad granite (Zal Farhad, 2014), Astaneh granite (Tahmasbi Zahra *et. al.*, 2009) Molla Taleb pegmatites (Mansouri and Khalili 2014), Alvand plutonic complex (Sepahigero *et. al.*, 2014), Ganjnameh and Mangavai Pegmatites (Ahmadi *et. al.*, 2016), Nehbandan Pegmatites (Ahmadi Bankdar, Ahmadi, 2014, yazdi et al, 2017 and 2019), Boroujerd region (Mirsepehvand *et. al.*, 2011), Shah Kooh granite (Ismaili *et. al.*, 2004), quartz diorites of Shurab region (Gholami *et. al.*, 2016), Adarba area in the northeast of Golpayegan (Mirlohi, Khalili, 2016), and Kuh Zar Au-Cu mine (Semnan) (Khalili, Mackizadeh, 2012., Bazoobandi *et. al.*, 2016). According to research in these areas, tourmalines belong mostly to the Dravite-

Schorl series and form in different conditions from magmatic to hydrothermal. Also, studies on tourmalines in the area of Molla Taleb have shown that these tourmalines are of the Schorl type and are associated with metamorphic or metasomatic assemblies. Tourmalines in the Zhan region (located 38 km east of Molla Taleb) have chemical zoning, are of Schorl type, and have a magmatic origin (Moradi *et. al.*, 2017). In the present study, using microprobe analysis and ICP-MS data, the composition of tourmaline and controlling agents, the behavior of tourmaline REEs in pegmatite rocks of Molla Taleb are investigated and their type and origin in different units containing tourmaline are identified.

### STUDY METHOD

Initially, to determine the composition, type, and origin of tourmaline in different units containing tourmaline in the area of Molla Taleb, 11 samples of pegmatites containing tourmaline nodules, tourmaline veins, and aplite veins were selected to prepare smooth thin sections and detailed mineralogical studies and determination of suitable minerals for analyzes related to mineral chemistry. In the Mineral Processing Research Center of Iran, microprobe analysis of the desired minerals was performed using the point analysis device (Cameca SX10 model, made by Cameca Company, France). In this analysis, tourmaline minerals were analyzed at 18 points under a 15-keV accelerator voltage and 20 nA current intensity. To determine the RREs as cations and also to determine the 10 main oxides by XRF and ICP-MS methods, 59 samples of host rock and 2 samples of tourmaline mineral were analyzed in the laboratory. To separate the tourmaline mineral, after crushing, the tourmaline samples were passed through the bromoform solution, followed by separating the tourmaline grains and purifying them using a binocular microscope. Silicate jadeite standards were used for sodium, enstatite for magnesium, Fayalite for iron and manganese, Apatite for phosphorus, Wollastonite for calcium, and alkaline feldspar for sodium and aluminum (Table 1).

Table 1. Microprobe electrons analysis of tourmalines in 11 samples of pegmatite rocks in Molla Taleb area based on 31 oxygen anions

Sample No.	1	2	3	4	5	6	7	8	9	10	11
------------	---	---	---	---	---	---	---	---	---	----	----

SiO <sub>2</sub>	34.32	34.53	35.22	33.98	33.54	34.24	34.29	34.14	34.41	34.3	34.24
TiO <sub>2</sub>	0.73	0.78	0.82	0.69	0.88	0.95	0.95	0.7	0.71	0.75	0.65
Al <sub>2</sub> O <sub>3</sub>	35.14	35.02	32.55	35.4	34.85	33.02	35	34.56	35.1	35.19	34.86
V <sub>2</sub> O <sub>3</sub>	0	0.06	0.05	0	0.07	0.07	0.06	0.05	0.05	0.05	0.03
FeO	13.32	13.3	9.66	13.24	13.8	10.65	12.94	13.84	13.58	14.09	13.85
MgO	0.7	0.61	5.1	0.56	0.69	3.81	0.74	0.86	0.69	0.53	0.7
CaO	0.16	0.22	0.83	0.21	0.22	0.88	0.19	0.21	0.18	0.18	0.19
MnO	0.16	0.16	0.11	0.17	0.13	0.1	0.12	0.17	0.2	0.2	0.19
Na <sub>2</sub> O	1.56	1.56	1.97	1.52	1.69	1.72	1.7	1.59	1.69	1.74	1.75
K <sub>2</sub> O	0.02	0.05	0.04	0.05	0.04	0.04	0.03	0.05	0.02	0.04	0.03
F	0.6	0.31	0	0.6	0.62	0	0.17	0.06	0	0.41	0.59
H <sub>2</sub> O*	3.30	3.45	3.63	3.29	3.26	3.58	3.51	3.54	3.60	3.41	3.30
B <sub>2</sub> O <sub>3</sub> *	10.4	10.4	10.5	10.3	10.3	10.4	10.4	10.3	10.4	10.4	10.4
Li <sub>2</sub> O*	0.25	0.32	0.19	0.26	0.20	0.21	0.35	0.18	0.26	0.24	0.24
Total	100.6	100.8	100.7	100.3	100.3	99.6	100.4	100.3	100.9	101.6	101.0
T: Si	5.74	5.76	5.82	5.71	5.66	5.74	5.73	5.74	5.74	5.71	5.73
Al	0.26	0.24	0.18	0.29	0.34	0.26	0.27	0.26	0.26	0.29	0.27
B	3.00	3.00	3.00	3.00	3.00	3.00	3.00	3.00	3.00	3.00	3.00
Z: Al	6.00	6.00	6.00	6.00	6.00	6.00	6.00	6.00	6.00	6.00	6.00
Y: Al	0.68	0.65	0.16	0.71	0.60	0.27	0.63	0.59	0.64	0.62	0.61
Ti	0.09	0.10	0.10	0.09	0.11	0.12	0.12	0.09	0.09	0.09	0.08
V	0.00	0.01	0.01	0.00	0.01	0.01	0.01	0.01	0.01	0.01	0.00
Mg	0.17	0.15	1.26	0.14	0.17	0.95	0.18	0.22	0.17	0.13	0.17
Mn	0.02	0.02	0.02	0.02	0.02	0.01	0.02	0.02	0.03	0.03	0.03
Fe <sup>2+</sup>	1.86	1.86	1.34	1.86	1.95	1.49	1.81	1.95	1.89	1.96	1.94
Li*	0.17	0.21	0.12	0.18	0.14	0.14	0.23	0.12	0.17	0.16	0.16
ΣY	3.00	3.00	3.00	3.00	3.00	3.00	3.00	3.00	3.00	3.00	3.00
X: Ca	0.03	0.04	0.15	0.04	0.04	0.16	0.03	0.04	0.03	0.03	0.03
Na	0.51	0.50	0.63	0.49	0.55	0.56	0.55	0.52	0.55	0.56	0.57
K	0.00	0.01	0.01	0.01	0.01	0.01	0.01	0.01	0.00	0.01	0.01
X	0.46	0.45	0.21	0.46	0.40	0.27	0.41	0.43	0.42	0.40	0.39
OH	3.68	3.84	4.00	3.68	3.67	4.00	3.91	3.97	4.00	3.78	3.69
F	0.32	0.16	0.00	0.32	0.33	0.00	0.09	0.03	0.00	0.22	0.31
x/x+Na	0.48	0.47	0.25	0.48	0.42	0.33	0.43	0.45	0.43	0.41	0.41
mg/mg+fe	0.09	0.08	0.48	0.07	0.08	0.39	0.09	0.10	0.08	0.06	0.08
feo/feo+mgo	0.95	0.96	0.65	0.96	0.95	0.74	0.95	0.94	0.95	0.96	0.95
R1	0.53	0.54	0.78	0.53	0.59	0.72	0.59	0.56	0.58	0.59	0.60
R2	2.06	2.03	2.61	2.02	2.14	2.46	2.01	2.19	2.09	2.12	2.14
R3	7.05	7.02	6.48	7.12	7.08	6.69	7.05	6.97	7.02	7.03	6.99

Structural formula based on 31 anions (O, OH, F)

## GENERAL GEOLOGY

Molla Taleb granitoid mass with coordinates of longitude 33° 49' to 40° 49' E and latitude 27° 33' to 39° 33' N is located in Varcheh 1:100000 sheet and Lacan

1:50,000 sheet in the western part of metamorphic SSZ in the northeast of Aligudarz city (Lorestan province) (Figure 1). Based on U-Pb dating on zircon mineral (Esna-Ashari *et. al.*, 2011), it seems that this granitoid mass is concurrent with the granitoid masses of Boroujerd (Khalaji *et. al.*, 2006, 2007) Astaneh (Masoudi *et. al.*, 1997, 2002, Poorbehzadi *et. al.*, 2019), and Alvand (Sepahigero *et. al.*, 2014) in the Middle Jurassic period. It has penetrated schists and phyllites and caused adjacent metamorphism that begins with stained schists and ends in hornfels and migmatites (Lotfi, Shahrokhi, 2003; Shahrokh, 2009) (Figure 1).

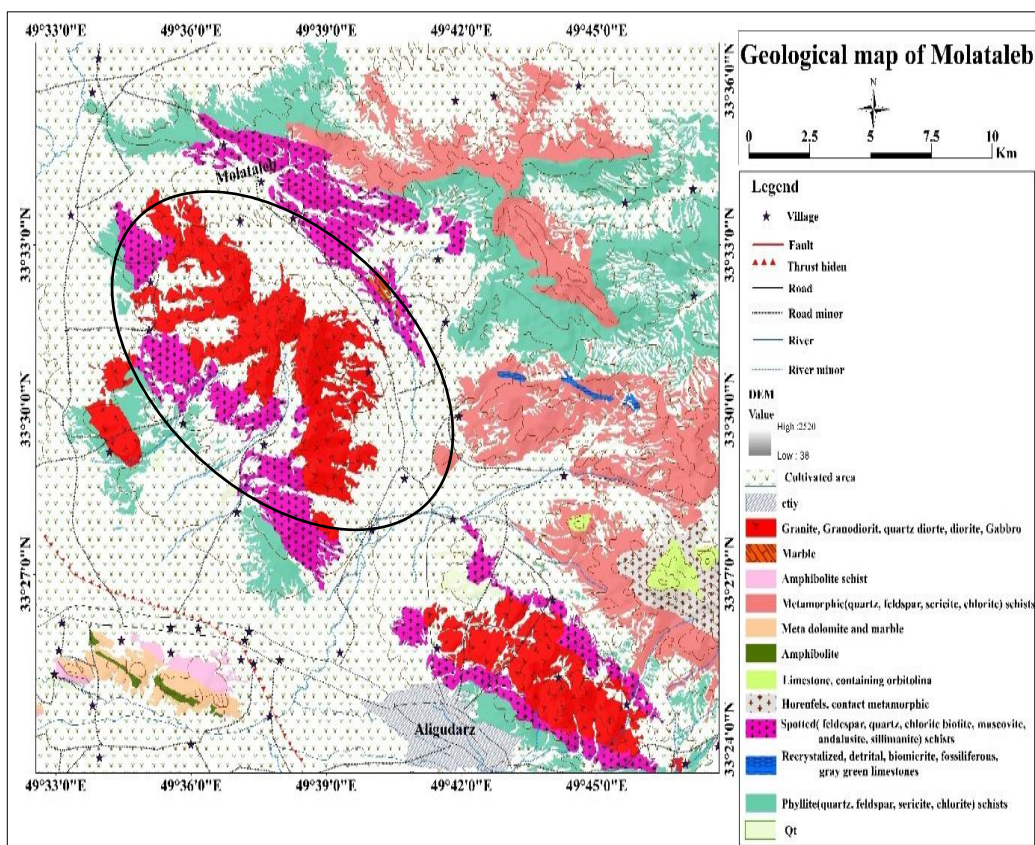
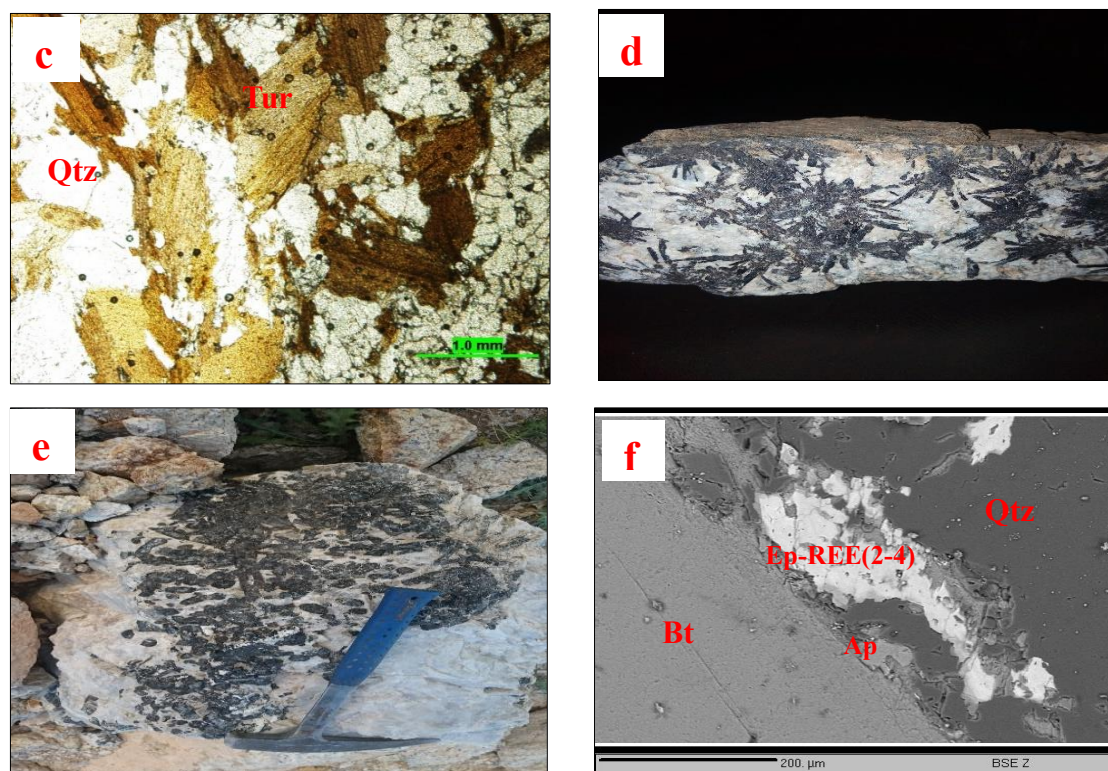


Figure 1. Geological map of the study area taken from 1: 100000 maps of Varche (Vaezipour and Kholqi 2004) and Aligudarz (Soheili *et. al.* 1992) (Geological survey and mineral exploration of Iran).

Following the field surveys on the rocks of the study area (granite and metamorphic assemblages), the relationship between aplite and pegmatite veins with these assemblages and the relationship of quartz-tourmaline veins with the host rock of granite, granodiorite and quartz diorite were studied. Field studies have shown that granites, quartz diorites, and granodiorites are the hosts of tourmaline-containing units in different parts of the area.

Molla Taleb granitoid mass with pegmatite texture contains tourmaline minerals (with a pale green to bright yellowish green and zonal structure), quartz, muscovite, plagioclase with polycystic twinning and epidote (Delfani Hossein, 20017). Molla Taleb tourmalines have outcrop in aplite veins and various pegmatite veins in granitoid masses as fine-grained and coarse-grained, respectively (Figure 2 a). In the Molla Taleb area, tourmaline-containing pegmatite and aplite-pegmatite veins have also outcropped in granodiorite rocks. They are fine-grained minerals formed in the middle of veins surrounded by silica and feldspar (Figure 2 b). These tourmalines are often fed by thin veinlets and can be the result of a boron-rich phase in the final phases. Solar tourmalines in the study area are scattered and sometimes dense. They overlap on the surface of joints in the host rock and usually around nodular tourmalines (Figure 2c). Based on microscopic observations, these types of tourmalines are often amorphous and show dark green to dark brown multicolor. They are surrounded by quartz and feldspar with a granular texture. These tourmalines also show poor zoning (Figures 2d and 2e). Sometimes, nodular tourmaline with quartz is observed in these granites, which in the hand sample have a dark center and light margins. This color change is due to ion exchange between the center and the margin of the tourmaline nodules, which leads to greater stability of the nodule center compared to its margin. Muscovite and sometimes feldspar inclusions are observed within the tourmaline coarse crystals. The nodules vary in shape, but the most common are spherical. In some cases, feldspar and tourmaline can be seen together in two completely separate sets (Figure 2f).





**Figure 2:** a) Field image of pegmatite containing coarse-grained tourmaline (Pirdadeh Beyranvand, 2020) b) Pegmatite and tourmaline-containing aplite-pegmatite veins outcropped in granodiorite (eastward view) (Pirdadeh Beyranvand, 2020) c) Microscopic image of vein tourmaline with quartz and feldspar in PPL light (Pirdadeh Beyranvand, 2020) d) Field image of solar tourmaline (Pirdadeh Beyranvand, 2020) e) Feldspar and tourmaline in two completely separate phases next to each other (southwest view) (Pirdadeh Beyranvand, 2020) and f) Microprobe electron image of tourmaline with quartz and plagioclase (Pirdadeh Beyranvand, 2020).

## PETROLOGY

In the study area, tourmaline-containing rocks have a light gray color with a Leucocratic color coefficient. Its main minerals are quartz (20%), plagioclase (20%), alkaline-feldspar (orthosis) (32%), and biotite (5%) and its accessory minerals are apatite, sphene, and tourmaline (27%). Alkaline-feldspar and plagioclase along with biotite have been subjected to severe alteration so that saussuritization and sericitization are obvious. Epidote is also the result of the decomposition of mafic minerals such as biotite, which are obtained along with iron oxides. For the chemical naming of the studied rocks, the diagrams provided by the Middlemost (1994) and De La Roche *et. al.* (1980) were used.

The studied rocks are in the range of gabbro, diorite, granodiorite, and granite (Figures 3a and 3b). In differentiation diagrams of magmatic series (Miyashiro, 1974; Hastie *et. al.*, 2007; Irvine, Baragar, 1971), the specimens are mostly in the calc-alkaline range (Figures 3c, 3d, and 3e). According to the A/CNK versus A/NK diagram, the selected samples are mainly peraluminous in composition (Shand, 1943) (Figure 3f).

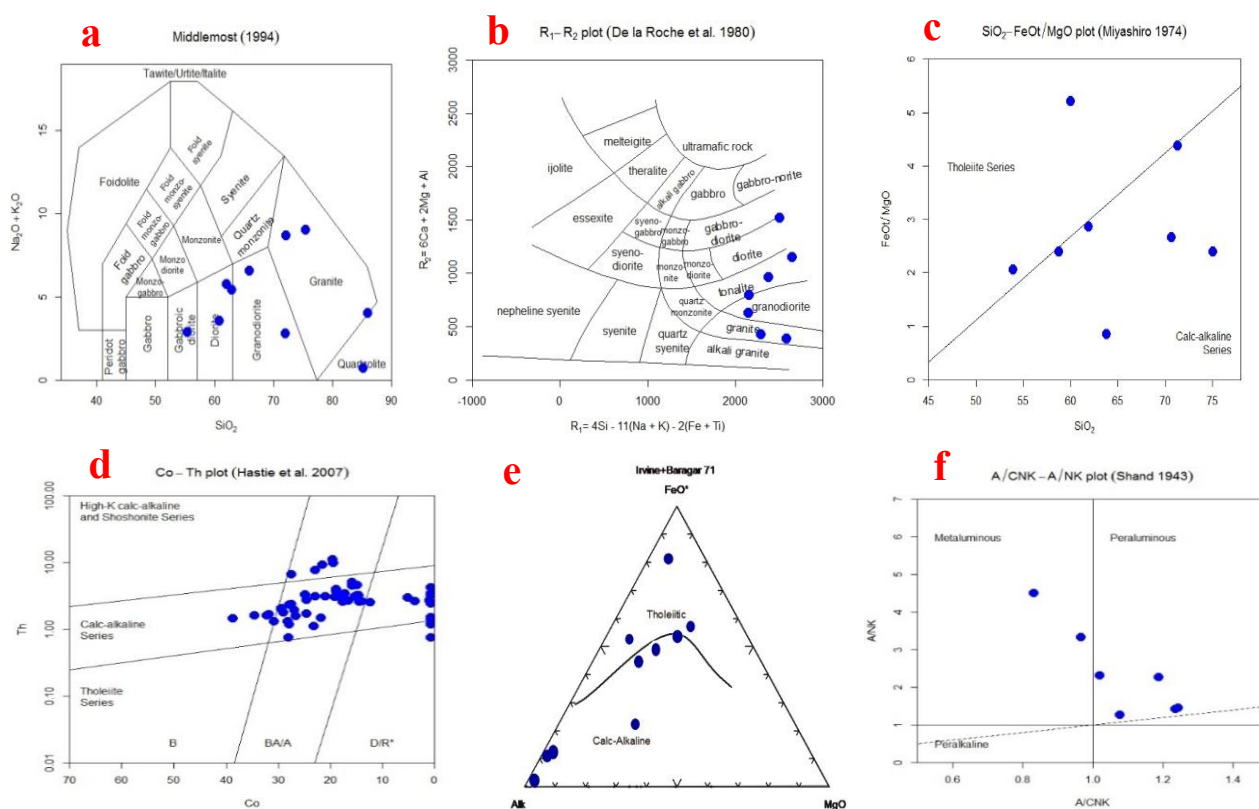


Figure 3. a) Position of the studied samples on a) the Na<sub>2</sub>O + K<sub>2</sub>O/SiO<sub>2</sub> diagram(Middlemost, 1994) b) the R<sub>1</sub>-R<sub>2</sub> diagram(De la roche et al, 1980) c) SiO<sub>2</sub>-FeO/MgO diagram(Miyashiro, 1974) d) Co-Th diagram(Hastie et al, 2007) e) AFM diagram(Irvine & Baragar, 1971) f) and A/CNK vs. A/NK diagram(shand, 1943).

Na<sub>2</sub>O versus SiO<sub>2</sub> diagrams (Chappell, White, 2001) and Ga-Al<sub>2</sub>O<sub>3</sub> diagrams (Newberry *et. al.*, 1990) were used to separate type-A and type-IS granites. The studied granites are mostly in the range of type-I granites (Figures 4a and 4b). To determine the degree of enrichment of the source of igneous rocks in the region, the ratios of incompatible elements Nb-Zr presented by Sun and McDonough (1989) were used to separate the enriched sources from the depleted sources. Due to their very low mobility, even at high degrees of alteration, these elements are very useful for the interpretation of altered

samples diagenesis. Accordingly, most of the samples in the study area are taken from the enriched range (Figure 4c). To determine the tectonic environment, diagrams of sub-elements because of immobility were used due to hydrothermal processes. According to the diagrams (Figures 4 d, 4e, and 4f), the studied samples are in the range of the volcanic arc and coincide with the collision (Pearce *et. al.*, 1984).

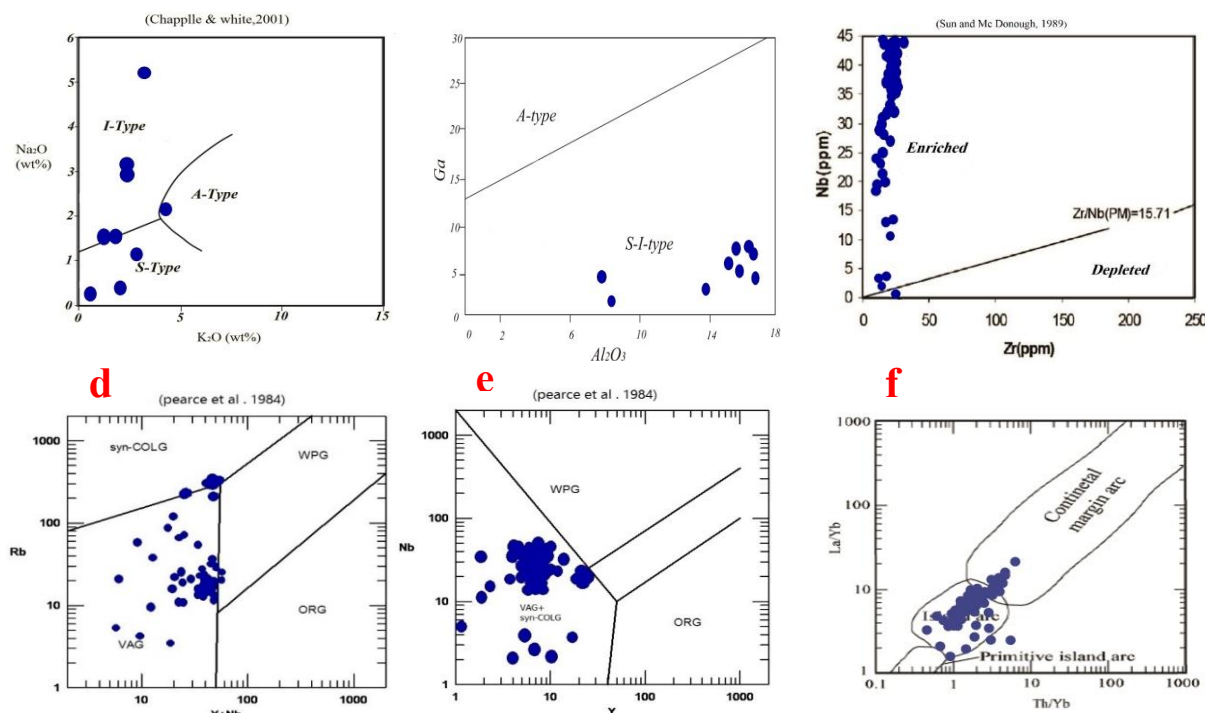


Figure 4. Position of the studied samples on a) the Na<sub>2</sub>O-K<sub>2</sub>O diagram (Chappelle and White, 1974, 2001) b) the Ga-Al<sub>2</sub>O<sub>3</sub> diagram (Newberry *et al.*, 1990) c) the Nb-Zr diagram (Sun & McDonough, 1989) d) the Rb-Y + Nb diagram (Pearce, *et. al.* 1984) e) the Nb-Y diagram (Pearce, *et al.*, 1984) and f) the La/Yb diagram versus Th/Yb (Condi, 1989).

In the study of REE distribution pattern based on spider diagrams, the values of incompatible and rare earth elements in the samples of the region are normalized to the values of chondrite (Thompson, 1982) (Figure 5a), primary mantle (Sun, McDonough, 1989) (Figure 5 b), the upper crust (Taylor, McLennan, 1985) (Figure 5 c), and the lower crust (Weaver, Tarney 1984) (Figure 5 d). In these diagrams, the elements Th, Rb, Cs, Nb, Eu, and Pb U are enriched and elements such as K, Ti, Sr, Ba, P, and Y are depleted. In spider diagrams, where REEs are normalized to chondrite (Thompson, 1982), negative anomalies of P and Ti are seen, which are specific to arcuate calc-alkaline volcanic massifs. The high concentrations of Th and Rb and the decrease of Sr and Ti are consistent with the values of crustal melts and

indicate some crustal contamination during magmatic transformations (Masoudi *et al.*, 2002). Enrichment in LILE elements (Cs, Th, and Rb) and Pb and depletion in phosphorus are evident in most samples. Such a pattern is one of the geochemical characteristics of magma present at the subduction site or the participation of the magmatic crust in the magma genesis. Also, the negative anomaly of high field strength elements (HFSE) such as Ti and P and the positive Pb anomaly suggest a continental arc setting for these rocks (Wilson, 1989).

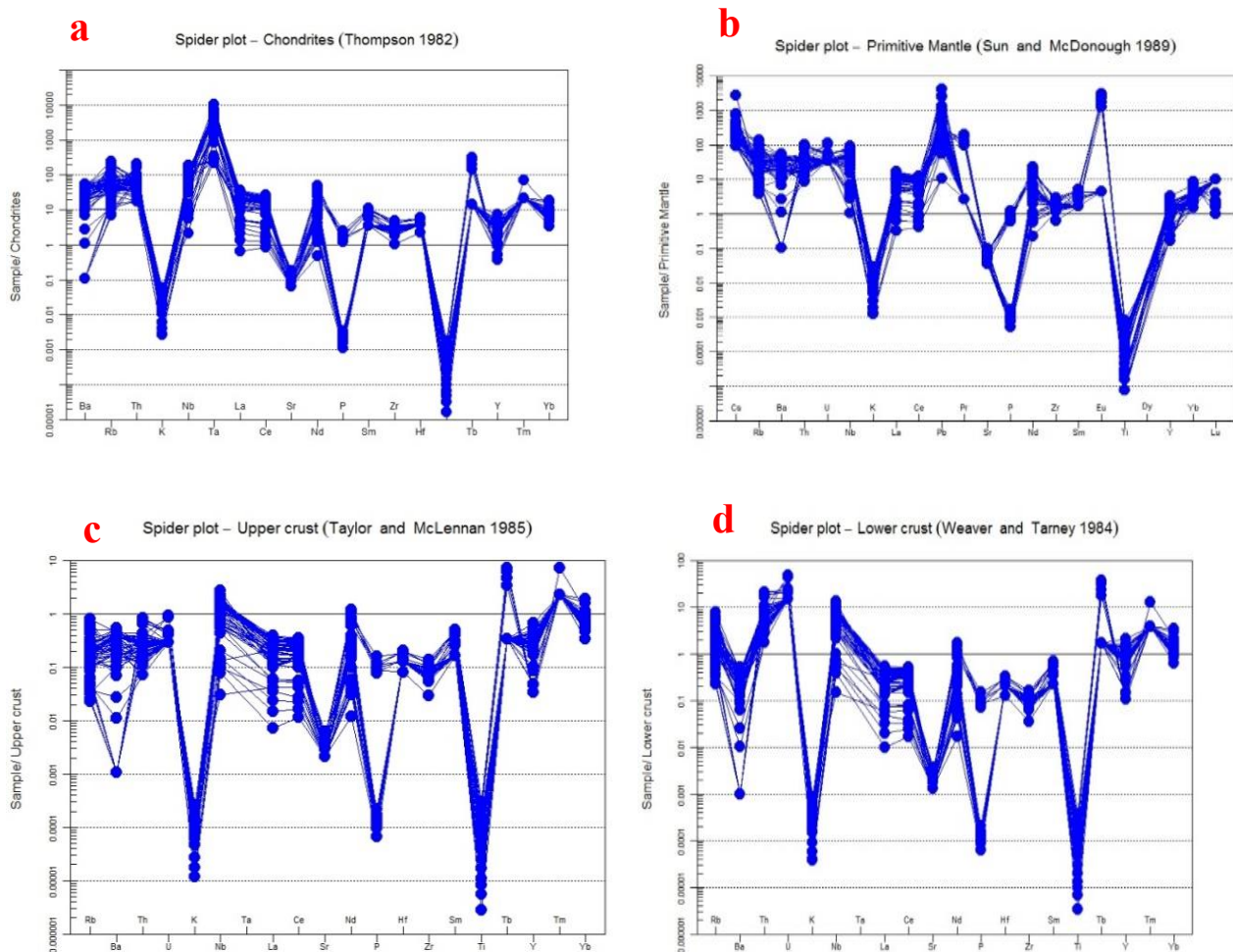


Figure 5. Normalized rare element patterns relative to a) chondrite(Tompson, 1982) b) primary mantle(Sun and Mc Donough, 1989) c) N upper crust(Tylor and Mc Lennan. 1985) and d) lower crust(Weaver and Tarney, 1983).

**THE MINERAL CHEMISTRY OF TOURMALINE**

Data related to microprobe analyzes of tourmaline minerals in the study area are presented in Table 1 and the structural formula is calculated based on 31 anions. To study

the type of tourmalines, a binary diagram of X-vac / X-vac + Na versus Mg / Mg + Fe (Hawthorne, Henry, 1999) was used (Figure 6a). According to this chart, all tourmalines were in the range of Schorl. Tourmalines are divided into three categories of calcium, alkaline, and those with vacant x-position. This classification is based on the presence or absence of space at position X and the values of Ca, Na, K (Hawthorne, Henry 1999). Based on this classification, samples were taken from tourmaline-containing aplite-pegmatite veins and nodular tourmalines. Most tourmalines in pegmatites in the ternary diagram of Ca Na + K, X-Vac (Hawthorne, Henry 1999) are in the range of alkaline tourmalines (Figure 6 b). According to the diagram R1 + R2 versus R3 (Maning, 1982), in these tourmalines, the substitution is of alkaline-deficiency type and position Y is not filled. The deficiency in this position is explained by the replacement of some of the existing Mg and Fe by Al and Li in position Y (Figure 6c). The Fe diagram versus Mg (London, Maning 1995) was used to investigate position Y in the tourmaline mineral. In this diagram, the changes of Fe versus Mg of the Schorl-Dravite combination places above the line  $\Sigma (Fe + Mg) = 3$ . Therefore, most of the samples are below line  $\Sigma (Fe + Mg) = 3$ , and all samples with  $\Sigma (Fe + Mg) < 3$  show the substitution of Al at position Y. In this regard, London and Maning (1995) believe that with a decrease in  $\Sigma (Fe + Mg)$ , the Al substitutions in position Y increased, suggesting the existence of substitutions of the empty X position and aluminum instead of sodium and iron in tourmalines. According to this diagram, all samples taken from tourmalines in the study area have  $\Sigma (Fe + Mg) < 3$  and less Mg than Fe. So, they are located in the Schorl region (Figure 6d).

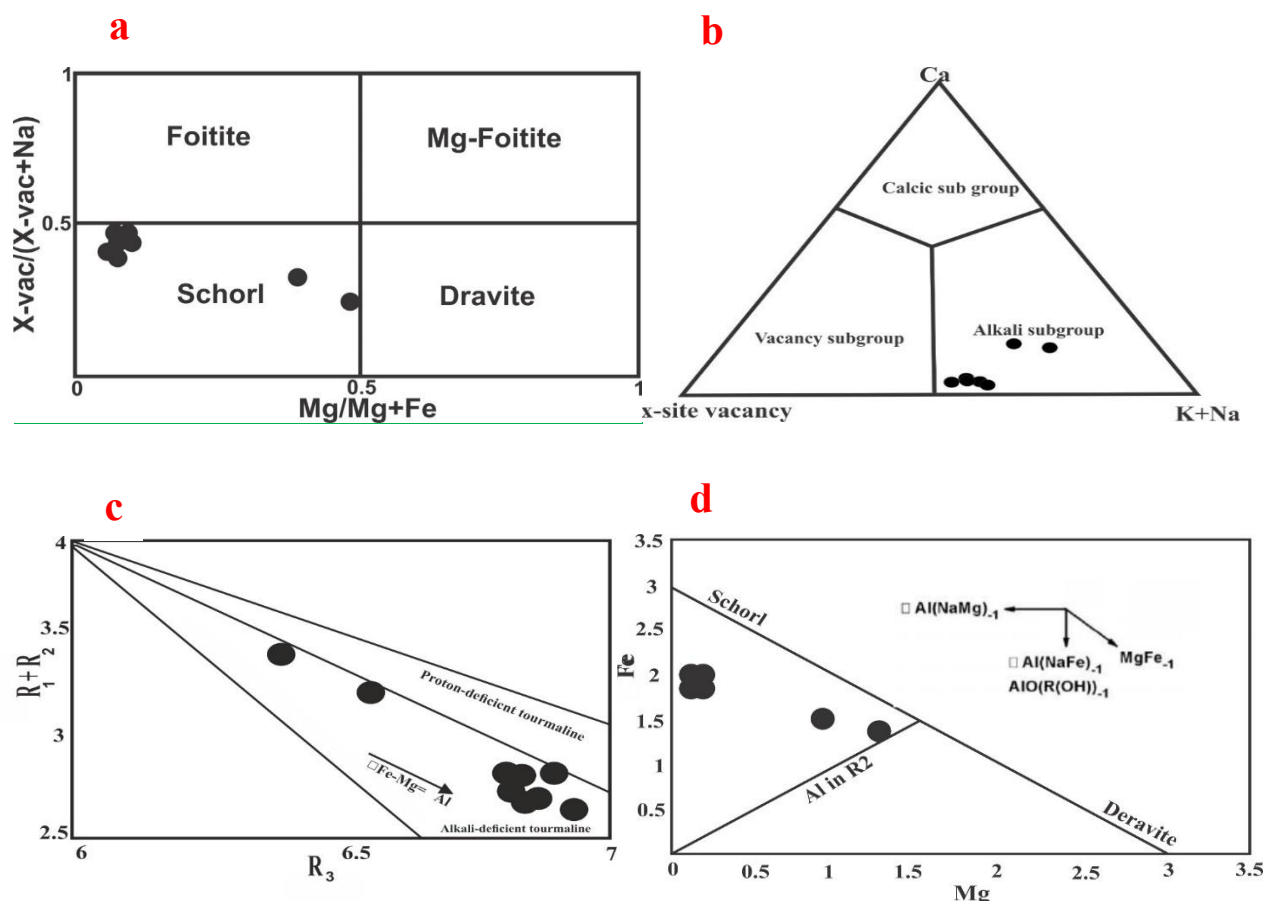


Figure 6. a) Diagram of  $X_{vac} / X_{vac} + Na$  versus  $Mg / Mg + Fe$  (Slack, 1993) b) Ternary  $Ca-Na + K-X_{vac}$  (Hawthorne & Henry, 1999) c)  $R_1 + R_2$  versus  $R_1 = Ca + Na$ ,  $R_2 = Fe + Mn + Mg$ , and  $R_3 = Al + 1.33Ti$  (Maining, 1982) and d)  $Fe$  versus  $Mg$  (London & Maining, 1995).

## DISCUSSION

Molla Taleb pegmatites can be divided into different units varying from granite to granodiorite during their evolution. In this mass, low-level tourmalinization is observed mainly in the granite unit. Molla Taleb granite mass, which is a type-I granite, is the result of the melting of the lower crust and has been contaminated with the upper crust during its evolution. Tourmalines in granites are self-forming and without zoning. They are crystallized under conditions of being peraluminous ( $1 A / CNK >$ ),  $PH < 6.5$ , and  $B_2O_3 = 2 \text{ wt.}\%$  (Pesquera *et. al.*, 1999). Also, magmatic tourmalines have higher Al content and more deficiency in X position compared to hydrothermal tourmalines (Trumbull, Chaussidon, 1999). According to Figs. 6c and 6d, all tourmalines have high Al concentration and decrease at X position and are of magmatic origin. Magmatic tourmalines also have higher Fe / Fe + Mg iron content

than hydrothermal tourmalines. Accordingly, the magmatic nature of the tourmalines in the Molla Taleb area can be confirmed using the collected samples. Besides, a high ratio of Fe+2 to Mg in tourmaline indicates its magmatic melt origin (Cavarretta, Puxeddu, 1990).

Therefore, the tourmalines present in the Molla Taleb area are magmatic. The tourmalines studied are in the Schorl-Darvite solution series and tend to have a high magnesium content. These tourmalines are among the alkaline tourmalines. To determine the source rock of the studied tourmalines, the ternary Al-Fe-Mg and Ca-Fe-Mg diagrams (London, Maning, 1995) are used. Based on these diagrams, the studied tourmalines were in the range of lithium-rich granitoids, pegmatites, and aplite and one of the samples was in the range of quartz-tourmaline rocks, calcium-poor meta-psammite, and meta-pelite. This is due to the presence of more magnesium in the samples, which shifts them from the category of granitoids to meta-pelite (Figure 7).

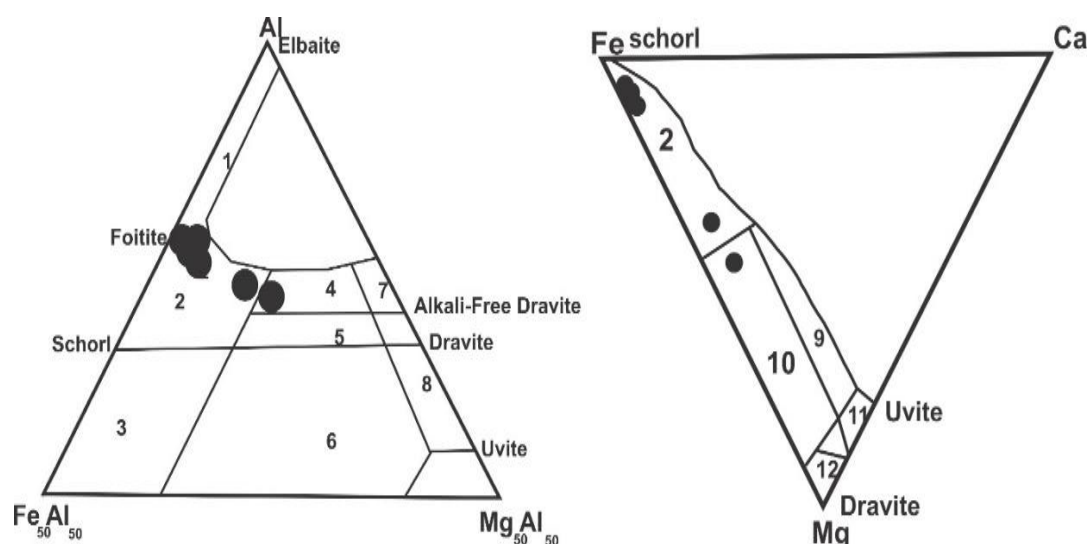


Figure 7. Ternary diagrams of Al-Fe-Mg and Ca-Fe-Mg (1: Lithium-rich granitoids, pegmatites, and the related aplite, 2: Lithium-depleted granitoids, pegmatites, and the related aplite, 3: Quartz-tourmaline rocks rich in Fe<sup>3+</sup>, 4: Coexisting meta-psammite and meta-pelite with an aluminum-saturated phase, 5: Non-coexisting meta-pelite and metapsamites with a saturated phase of aluminum, 6: Calc-silicate rocks, meta-pelite, and quartz-tourmaline rocks rich in Fe<sup>3+</sup>, 7: Low-calcium metamorphic ultramafic and vanadium and chromium-rich metasediments, 8: Metacarbonates and metapyroxenites, 9: Calcium-rich meta-pelite and metapsamites, 10: Quartz-tourmaline rocks, calcium-poor meta-pelite, and metapsamites, and 11: Metacarbons 12. Metamorphic ultramafic)(London & Maining, 1995).

Under hydrothermal conditions, tourmaline is produced in much lower amounts of B and a wider range of compounds compared to the magmatic conditions (Weisbrod *et al.*,

1986). The tourmalines of pegmatite veins are probably formed as magmatic form due to their location in the granitoid region. These veins are formed after the penetration of the main granite mass due to the re-penetration of magma and its injection into the main mass. Molla Taleb granitoid complex is chemically peraluminous (Esna-Ashari *et. al.*, 2011). Therefore, it can provide the amount of Al necessary for the formation of tourmaline within the mass and aplite-pegmatite veins. The presence of early tourmalines also indicates that the granitoid mass had the required amount of B to form tourmaline within the mass and in the veins. Moreover, considering the value of  $FeO + MgO > 10$  in this mass, it can be said that there are enough Mg and Fe for the formation of tourmaline. As a result, the origin of Mg, Fe, Al, and B required for the formation of tourmaline in the granitoid mass should be considered. Closure of the magmatic system, non-interference of fluids, and contamination of them with Al-rich sediments in tourmaline are identified by  $Fe = FeO / FeO + MgO > 0.8$ . However, when  $Fe = FeO / FeO + MgO$  is less than 0.6, it indicates boron metasomatism with Al-rich sediments and boron from an external source. The diagram of  $FeO / FeO + MgO$  versus MgO (Figure 6) was used to determine the magmatic system of tourmalines (Pirajno and Smithies 1992). This diagram introduces three magmatic, magmatic-hydrothermal, and hydrothermal systems for tourmaline formation. According to this diagram, some tourmalines with  $FeO / FeO + MgO$  ratios between 0.6 and 0.8 are in the magmatic-hydrothermal range, indicating the combined effect of both magmatic and hydrothermal processes in their formation. But some other samples with  $FeO / FeO + MgO$  more than 0.8 are in the range of magmatic tourmalines. This ratio for some tourmalines is more than 0.8. It shows that boron originates from magmatic fluids in the late stages, which is of magmatic type in the tourmalines in the study area. Besides, the amount of  $Fe = FeO / (FeO + MgO)$  of tourmaline decreases with increasing the distance from the granitic mass of the hydrothermal fluid. This ratio is between 0.8 and 1 for the granitic deposits attached to the granite mass and less than 0.6 for vein systems at a distance equal to or greater than 1 km (Pirajno, Smithies, 1992).

Considering the ratio of  $\text{FeO} / (\text{FeO} + \text{MgO})$  from different samples of Molla Taleb, some of which are higher than 0.8 and the location of some samples is in zone A (Figure 8), it can be concluded that the distance of tourmaline veins in the study area from Aligudarz granite massif was less than 1 km. Therefore, the effect of metamorphic units on the formation of tourmalines in the region is negligible due to their Fe content and also their location in the range of lithium-poor granitoids, pegmatites, and aplite related to them (Figure 8). The placement of some samples analyzed in zone A indicates the relatively high Fe content in these regions. It suggests the proximity of the tourmaline formation area to the fluid supply source and indicates a distance of less than 1 km from the intrusion mass.

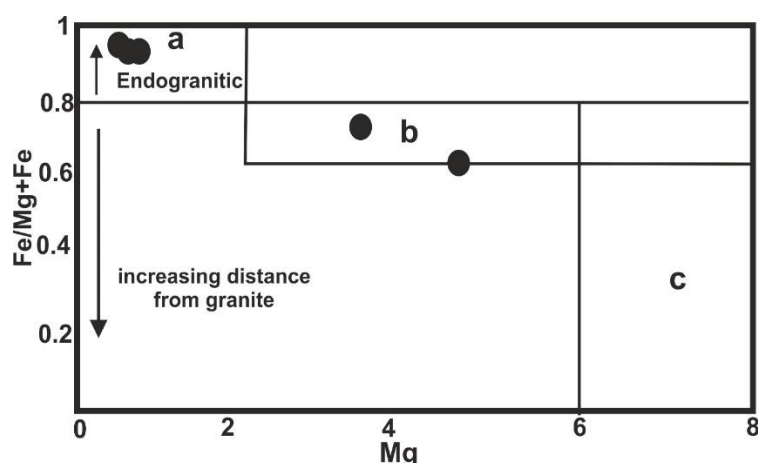


Figure 8.  $\text{FeO}/(\text{FeO} + \text{MgO})$  versus  $\text{MgO}$  diagram; the figure shows the territory of endogranite tourmalines up to Type-a granite mass, up to intermediate Type b granite mass, and tourmalines far from granite Type C (Pirajno, 1992).

## CONCLUSION

According to obtained results, the studied rocks in the Molla Taleb area are in the range of gabbro, diorite, granodiorite, and granite. In the diagrams of the magmatic series differentiation, the samples taken are mostly in the calc-alkaline range and mainly have a peraluminous composition. To determine the enrichment degree of the source of igneous rocks in the region, the ratios of incompatible elements Nb-Zr were used to detect the enriched sources from the depleted ones. Most of the samples in the study area are in the range of depleted mantle. To determine the tectonic setting according to the diagrams, the studied samples are located in the volcanic arc range and at the same time with the collision.

The occurrence of tourmaline in the Molla Taleb granite mass, regarding its type-I nature, can be due to the contamination of the magma melted from its lower crustal with the upper crust and the increase in aluminum saturation. Hence, the origin rock of tourmaline can be attributed to a range of granitoids rich in lithium, pegmatites, and their associated aplite.

The studied tourmalines are generally in the range of Schorl-Dravite series with a tendency towards magnesium-rich compounds (magnesium-rich Schorl and Dravite) and alkaline. In the diagram of Mg versus Fe/Fe + Mg, tourmaline-containing aplite-pegmatite veins, nodular tourmalines, and quartz-tourmaline veins have the highest amount of magnesium and tourmalines in pegmatites have the highest amount of Fe / Fe + Mg and the lowest amount of Mg. Placement of all samples below  $\Sigma (Fe + Mg) < 3$  indicates the substitution of Al in position Y. The presence of self-formed tourmalines in the granites of this area, the absence of chemical zoning, and the observation of tourmalines in various forms, including nodules indicate that the magma of the origin of these granites is rich in B. Tourmalines, which are embedded in pegmatites or the form of aplite and pegmatite veins, are of magmatic origin. In comparison, hydrothermal tourmalines (late magmatic) are present in meta-aluminous granite host rocks (quartz diorites). Thus, it seems that the origin of boron in different units is of magmatic or hydrothermal type. The ratio of  $FeO = FeO / FeO + MgO$ , which is more than 0.8 in tourmaline areas, shows that boron originates from magmatic fluids in the late stages.

## REFERENCES

- ABU EL-ENEN M. M., OKRUC M.; The texture and composition of tourmaline in metasediments of the Egypt, Implication for the tectono-metamorphic evolution of the Pan-African basement. **Mineralogy Magazine**, 71(1), 2007. p.17-40.
- AHMADI BANKDAR, S.; AHMADI A. Tourmaline composition in Chah Rouii pegmatites, southwest of Nehbandan. **Journal of Crystal and Mineralogy**, v. 21, n. 32, 014. p. 549-560.
- AHMADI, K. A. **Petrology of granitoid rocks in Boroujerd region**, Ph.D. thesis in Petrology, Faculty of Science, University of Tehran, 2006, 190 p.
- AHMADI, K. A.; TAHMASEBI, N. Z.; ZAL, F.; SHABANI, Z. Behavior of the main and rare elements of tourmaline mineral in Mangavi and Ganjnameh pegmatites (Hamadan region). **Petrology**, v. 7, n. 27, 2016. p. 1-24.

- AHMADI-KHALAJI A.; ESMAEILI D.; VALIZADEH M. V.; RAHIMPOUR-BONAB, H. Petrology and Geochemistry of the Granitoid Complex of Boroujerd, Sanandaj-Sirjan Zone, Western Iran. **Journal of Asian earth Sciences**, 29. 2007. p. 859-877.
- BARATIAN, M.; ARIAN, M. A.; YAZDI, A. Petrology and Petrogenesis of Siah Kooh volcanic rocks in the eastern Alborz. **GeoSaber**, 11, 2020. P. 349-363. doi: <https://doi.org/10.26895/geosaber.v11i0.980>
- BAZOOBANDI, M. H.; ARIAN, M. A.; EMAMI, M. H.; TAJBAKSH, G.; YAZDI, A. (2016). Petrology and Geochemistry of Dikes in the North of Saveh in Iran. **Open Journal of Marine Science**, 6, 2016. p. 210-222. doi: 10.4236/ojms.2016.62017
- BEA, F.; PEREIRA, M. D.; STROH, A. Mineral/leucosome trace-element partitioning in a peraluminous migmatite (a laser ablation-ICP-MS study). **Chemical Geology**, 117: 1994, p. 291-312.
- BURIÁNEK, D.; NOVÁK, M. Compositional evolution and substitutions in disseminated and nodular tourmaline from leucocratic granites: **Examples from the Bohemian Massif, Czech Republic. Lithos**, 95(1), 2007, p. 148-164.
- CAVARRETTA, G.; PUXEDDU, M. Schorl-Dravite-Ferridravite Tourmalines Deposited by Hydrothermal Magmatic Fluids during Early Evolution of the Larderchio Geothermal Field, Italy. **Economic Geology**, 85, 1990. p. 1236-1251.
- CHAPPELL, B. W.; WHITE, A. J. R. Two Contrasting Granite Types. **Pacific Geology**, 8, 2001. p.173-4.
- COPIJKOVA, R.; SKODA, R.; GALIOVA, M. V.; NOVAK, M. Distributions of Y + REE and Sc in tourmaline and their implications for the melt evolution; examples from NYF pegmatites of the Trebic Pluton, Moldanubian Zone, Czech Republic. **Journal of Geosciences**, 58(2), 2013. p. 113–131.
- DE LA ROCHE H.; LETERRIER, J.; GRANDCLAUDE, P.; MARCHAL, M. A classification of volcanic and plutonic rocks using R1R2-diagram and major element analyses-Its relationships with current nomenclature. **Chemical Geology**, 29, 183–210. 1980
- DELFANI, H. **Mineralogy, Geochemistry and Economic Geology of Feldspar and Tourmaline of Molla Taleb, North of Aligudarz city, Lorestan province**. Master Thesis of Islamic Azad University, Khorramabad Branch, 2017. 140 p.
- ESNA-ASHARI, A.; HASSANZADEH, J.; VALIZADEH, M. V. Geochemistry of microgranular enclaves in Aligoodarz Jurassic arc pluton, western Iran: implications for enclave generation by rapid crystallization of cogenetic granitoid magma. **Mineralogy and Petrology**, 101, 2011. p. 195–216.
- ESNA-ASHARI, A.; TIEPOLO, M.; VALIZADEH, M. V.; HASSANZADEH, J.; SEPAHI A. S. Geochemistry and zircon U-Pb geochronology of Aligoodarzgranitoid complex, Sanandaj-Sirjan Zone, Iran. **Journal of Asian Earth Sciences**, 43, 2012. p. 11-12
- FOIT, F. F.; ROSENBERG, P. E. Coupled substitutions in the tourmaline group. **Contributions to Mineralogy and Petrology**, 62, 1977. p. 109-117.
- GALBRAITH, C. G.; CLARKE, D. B.; TRUMBULL, R. B.; WIEDENBECK, M. Assessment of tourmaline compositions as an indicator of emerald mineralization at the Tsa da Glisza Prospect, Yukon Territory, Canada. **Economic Geology**, 104, 2009. p. 713–731.

GHOLAMI, A. A.; MOHAMMADI, S. S.; ZARRINKOOB, M. H. Petrography, mineral chemistry of tourmaline, geochemistry, and tectonic setting of Tertiary igneous rocks in Shurab area (west of Khusf), Southern Khorasan. **Journal of Crystal and Mineralogy**, 24, (1), 2016; p. 189-204.

HASTIE A. R.; KERR A. C.; PEARCE J. A.; MITCHELL, S. F. **Classification of Altered Volcanic Island Arc Rocks using Immobile Trace Elements: Development of the Th–Co Discrimination Diagram. *Journal of Petrology*, p 2007, p 2341–2347.**

HAWTHORNE, F. C.; HENRY, D. J. Classification of the minerals of the tourmaline group. **European Journal of Mineralogy**, 11, 1999. p. 201-215.

IRVINE, T. N.; BARAGAR, W. R. A. A guide to the chemical classification of the common volcanic rocks. **Canadian Journal of Earth Science**, v. 8, 1971. p. 523-276.

ISMAILI, D.; VALIZADEH, M. V.; KANANIAN, A. Mineral chemistry of tourmaline in quartz-tourmaline veins of SHAH-KUH granite (Eastern Iran). **Journal of Science**, University of Tehran, v. 30,n. 2, 2004. p. 157-177.

KHALILI, K. H.; MACKIZADEH, M. A. The occurrence of tourmaline in Kuh Zar (Baghoo) Au-Cu mine, south of Semnan province. **Petrology**, 3(9), 2012. p. 57-70.

KRYNINE, P. D. The tourmaline group in sediments. **Journal of Geology**, 54, 1946. p. 65-87.

LONDON, D.; MANING, D. A. C. Chemical variation and significance of tourmaline from SW England. **Economic Geology**, 90, 1995. p. 495-519.

LOTFI, M.; SHAHROKHI, S. V. Investigating the factors controlling copper and gold mineralization in Kondor, Aligudarz region, and its relationship with geodynamic problems of Mastarun granitoid massif (northeast of Lorestan province), **7th conference of Iranian Geological Society**; University of Isfahan, September 4-6, 2003.

MANING, D. A. C. Chemical and morphological variation in tourmalines from the Hub Kapong batholith of peninsular Tailand. **Mineralogical Magazine**, 45, 1982. p. 139-147.

MANSOURI ISFAHANI, M.; KHALILI, M. Mineralogy and Mineral chemistry of Tourmaline and Garnet in Granitoids of Molla Taleb Village (North of Aligudarz) Northwest of Isfahan. **Journal of Crystal and Mineralogy**, v. 22, n. 1, 2014. p. 139-148.

MASOUDI, F. **Contact metamorphism and pegmatite development in the region SW of Arak, Iran.** Ph.D. Thesis, Leeds University, UK, 1997. 135pp.

MASOUDI, F.; YARDLEY, B. W. D.; CLIFF, R. A. Rb-Sr geochronology of pegmatites, plutonic rocks and a hornfels in the region southwest of Arak, Iran. Islamic Republic of Iran. **Journal of Sciences**, 13(3), 2002. p. 249-254.

MICHAEL, A. W.; HORST, R. M.; PHILIPP, S.; ANNA, G.; THOMAS, W.; DORRIT, E. J.; MATTHIAS, B.; GREGOR, M. Trace element systematics of tourmaline in pegmatitic and hydrothermal systems from the Variscan Schwarzwald (Germany): The importance of major element composition, sector zoning, and fluid or melt composition. **Chemical Geology**, 344, 2013. p. 73-90.

MIDDLEMOST, E. A. K. Naming Materials in the Magma/Igneous Rock System. **Earth-Science Reviews**, 37, 1994. p. 215-244.

- MIRLOUHI, A. S.; KHALILI, M. Petrography and geochemistry of tourmaline nodules from Aderba leucogranite (northeast of Golpaygan, Sanandaj-Sirjan area). **Journal of Petrology**, v. 7, n. 27, 2016. p. 191-205.
- MIRSEPAHVAND, F.; TAHMASEBI, Z.; SHAHROKHI, S. V.; AHMADI KHALAJI, A. Geochemistry and determination of the origin of tourmalines in Boroujerd region. **Journal of Crystal and Mineralogy**, v. 20, n. 2, 2011. p. 281-292.
- MIYASHIRO, A. Volcanic rock series in island arcs and active continental margins. **American Journal of Science**, v. 274, 1974. p. 321-355.
- MORADI, A.; SHABANIAN, N.; DAVOUDIAN DEHKORDI, A. R. Geochemistry of mylonitic tourmaline-bearing granite- gneiss pluton in the northeast of June mine, **JOURNAL OF ECONOMIC GEOLOGY SPRING-SUMMER**, 2017 , Volume 9 , Number 1 (16) ; Page(s) 13 To 14. v. 9, n. 1, 2017. p. 141-158.
- NEWBERRY, R. J.; BUNN, L. E.; SWANSON, S. E.; SMITH, T. E. Comparative petrological evolution of the Sn and W granites of the Fairbanks–Circle area, interior Alaska. *In*: HANNAH J. L.; STEIN H. J.(Eds). **Ore-Bearing Granite Systems**; Petrogenesis and Mineralizing Processes. Geological Society of America, 246, 1990. p. 121–142.
- PEARCE, J. A.; HARRIS, N. B. W.; TINDLE, A. J. Trace elements discrimination diagrams for the tectonic interpretation of granitic rocks. **Journal of Petrology**, 25, 1984. p. 956-983.
- PESQUERA, A.; TORRES-RUIZ, J.; GIL-GRESPO, P. P.; VELILLA, N. Chemistry and genetic implications of tourmaline and Li-F-Cs micas from the Valdeflores area (Caceres, Spain). **American Mineralogist**, 84, 1999. p. 55-69.
- PIRAJNO, F.; SMITHIES, R. H. The FeO/(FeO+ MgO) ratio of tourmaline: a useful indicator of spatial variations in granite- related hydrothermal mineral deposits. **Journal of Geochemical Explorations**, n. 42, 1992. p. 371-381.
- Pirdadeh Beyranvand, D., 2020. Mineralogy, Geochemistry and Economic Geology of Feldspar and Tourmaline Mulataleb North of Aligudarz County, Lorestan Province, **PhD Thesis, Islamic Azad University, North Tehran Branch**, 300 p.
- POORBEHZADI, K.; YAZDI, A.; SHARIFI TESHNIZI, E.; DABIRI R. Investigating of Geotechnical Parameters of Alluvial Foundation in Zaram-Rud Dam Site, North Iran. **International Journal of Mining Engineering and Technology**, 1(1), 2019. p. 33-44.
- SCAILLET, B.; PICHAVANT, M.; ROUX, J. Experimental crystallization of leucogranite magmas. **Journal of Petrology**, 36(3), 1995. p. 663–705.
- SEPAHIGERO, A. A.; SALAMI, S.; TABRIZI, M. Geochemistry of tourmalines in pegmatite and aplite dykes of Alvand plutonic complex and metamorphic rocks of the Hamadan region. **Journal of Crystal and Mineralogy**. v. 23, n. 3, 2014. p. 495-506.
- SHAHROKH, S. V. Genetic of Kondor copper and gold mineralization in Aligudarz area, Lorestan,Iran. **6th European congress on regional geoscientific cartography and information system**, Bologna, Italy, 2009.

- SHAND, S. J. **A/NK-A/CNK diagram, to determine the degree of saturation of alumina in igneous rocks of the study area.**, London The Eruptive Rocks (3rd.) Thomas Murby, John Wiley, New York, p. 444. 1943.
- SLACK, J. F.; TRUMBULL, R. B. Tourmaline as a recorder of ore-forming processes. **Elements**, n. 7, 2011,1993. p. 321-326.
- SOHEILI, M.; JAFARIAN, M.; ABDOLLAHI, M. **Geological map 1:100000 Aligudarz area with a brief description.** Geological Survey and Mineral Exploration of Iran, 1992.
- SUN, S.; MCDONOUGH, W. F. Chemical and isotopic systematic of oceanic basalts: implication for Mantel composition and processes. *In*: SAUNDERS A. D.; NORRY, M. J. (eds) **Magmatism in oceanic basins**, Geological Society: London - Special Publications 42 ,1989. p. 313-345.
- TAHMASEBI, Z.; AHMADI KHALAJI, A.; RAJAIEH, M. Tourmalinization in the Astaneh granitoid massif (south of Arak). **Journal of Crystal and Mineralogy**, v. 17, n. 3, 2009. p. 368-380.
- TAYLOR, S. R.; MCLENNAN, S. M. The continental crust: its composition and evolution. **Geoscience texts**, Blackwell Publishing: Oxford, 1985.
- THOMPSON, R. N. Magmatism of the British, Tertiary volcanic province. **Scottish Journal of Geology**, v. 18: 1982. p. 50-107.
- TORRES-RUIZ, J.; PESQUERA, A.; GIL CRESPO, P. P.; VELILLA, N. Origin and petrogenetic implications of tourmaline-rich rocks in the Sierra Nevada (Betic Cordillera, southeastern Spain). **Chemical Geology**, 197, 2003. p. 55-86.
- TRUMBULL, R. B.; CHAUSSIDON, M. Chemical and boron isotopic composition of magmatic and hydrothermal tourmalines from the Sinceni granite- pegmatite system in Swaziland. **Chemical Geology**,153, 1999. p. 125-137.
- VAEZIPOUR, M. H.; KHALQI, M. H. **Geological map 1:100000 Varcheh with a brief description.** Geological Survey of Iran, 2004.
- VAN HINSBERG, V. J. Preliminary experimental data on trace-element partitioning between tourmaline and silicate melts. **The Canadian Mineralogist**, 49, 2011. p. 153–163.
- WEAVER, B. L.; TARNEY, J. **Empirical approach to estimating the composition of the continental crust.** *Nature* **310**, 575–577 (1983)
- WEISBROD, A.; POLAK, C.; ROY, D. Experimental study of tourmaline solubility in the system Na-Mg-Al-Si-B-O-H. Applications to the boron content of natural hydrothermal fluids and tourmalinization process. Volume of Abstracts, **International Symposium Experimental Mineralogy and Geochemistry**, Nancy, 1986.
- WILSON, M.; **Igneous petrogenesis, a global tectonic approach.** Unwin Hyman: London, 1989.
- WOLF, M. B.; LONDON, D. Boron in granitic magmas: Stability of tourmaline in equilibrium with biotite and cordierite. **Contributions to Mineralogy and Petrology**, 130(1), 1997. p. 12–30.

YAZDI, A.; ASHJA-ARDALAN, A.; EMAMI, M. H.; DABIRI, R.; FOUDAZI, M. Chemistry of Minerals and Geothermobarometry of Volcanic Rocks in the Region Located in Southeast of Bam, Kerman Province. **Open Journal of Geology**, 7, 2017. P. 1644-1653. doi: 10.4236/ojg.2017.711110

YAZDI, A.; SHAHHOSINI, E.; DABIRI, R.; ABEDZADEH, H. Magmatic Differentiation Evidences And Source Characteristics Using Mineral Chemistry In The Torud Intrusion (Northern Iran). **Revista GeoAraguaia**, 9(2), 2019. p. 6-21.

ZAL, F. **Geochemistry and determination of the origin of tourmaline in granites (g2) of Mashhad**, Master Thesis, Faculty of Science, Lorestan University, 2014. 110 pages.